ЖУРНАЛ ФІЗИЧНИХ ДОСЛІДЖЕНЬ
т. 22, № 4 (2018) 4701(7 с.)

JOURNAL OF PHYSICAL STUDIES
v. 22, No. 4 (2018) 4701(7 p.)

DIELECTRIC PROPERTIES OF AQUEOUS CELLULOSE NANOCRYSTALS AND NANOFIBERS SUSPENSIONS

Oleh Hrebnov*, Lyudmila Matzui, Leonid Bulavin
Taras Shevchenko National University of Kyiv,
64, Volodymyrska St., UA–01601 Kyiv, Ukraine
**e-mail: orticort@gmail.com*
(Received July 24, 2018; in final form October 12, 2018)

Dielectric properties of hydrophobic nanoparticles suspensions are intensively investigated nowadays. However, few works investigate suspensions of hydrophilic nanoparticles. In the present work, we investigate the influence of hydrophilic cellulose nanocrystals (CNCs) and cellulose nanofibers (CNFs) on the dielectric properties of aqueous suspensions. Purity and chemical composition of the nanoparticles was characterized by EDX and FTIR spectroscopy. The results of dielectric measurements show a decrease in the relaxation time of the CNCs aqueous suspension, as compared with that of pure water; no significant change in the relaxation time was observed for the CNFs aqueous suspension. The findings indicate that a hydrophilic surface may accelerate the dynamics of water molecules.

Key words: cellulose nanocrystals; cellulose nanofibers; dielectric properties.

DOI: https://doi.org/10.30970/jps.22.4701

PACS number(s): 77.22.−d

I. INTRODUCTION

Cellulose is one of the most abundant natural materials, which is renewable, biocompatible and biodegradable [1, 2]. Cellulose nanoparticles have favourable properties, such as high mechanical strength, relatively low density, high aspect ratio and relatively large specific surface area. These properties open a wide spectrum of cellulose nanoparticle applications in science. A highly popular application of cellulose nanoparticles is film production [3]. Films are spreading the range of possible applications of cellulose nanoparticles. Due to their ability to undergo rapid and reversible changes in colour upon swelling it is proposed to use the films for pressure sensing [4]. Also, biocompatible cellulose-based films in association with other materials open the perspective of its application in healthcare [5]. In combination with essential oils chitosan-carboxymethyl the cellulose films exhibit antifungal properties; therefore it is proposed to use this ecofriendly material in food industry for food preservation, to enhance food safety and quality [6]. Besides, cellulose nanoparticles are used for the creation of microcapsules with permeable membrane [7, 8, 9], production of energy storage devices, sportswear, lightweight armour and more [2].

The properties of cellulose nanoparticles depend on the production method. An important step in the production of cellulose nanoparticles is the preparation of aqueous suspensions. The properties of the aqueous suspensions, such as pressure or temperature, affect the properties of the resulting nanoparticles. So, it is important to understand the relation between the properties of the aqueous suspensions and the properties of the nanoparticle. One of the features ensuring intensive interactions between cellulose nanoparticles and water is a developed network of hydrogen bonds on the cellulose nanoparticle surface. The network of hydrogen bonds confines water molecules creating a water shell, which has properties other than those of bulk water [10, 11]. A large body of research is dedicated to studying the water shell properties of molecules or nanoparticles [12, 13, 14].

A common method for the confined water investigation is a dielectric relaxation spectroscopy [15, 16]. The dielectric spectra are characterized by maximums corresponding to different relaxation processes in a system (so-called α, β, γ, δ-relaxation, etc.). The water relaxation process is manifested at frequencies of the order of GHz (β-relaxation), therefore we investigate the dielectric properties of the suspensions in a frequency range of 1 to 30 GHz.

Various water mixtures were investigated in this range of frequencies, for example, with ethanol [17], peptides [18], lysosomes [19], or metal nanoparticles [20]. Usually, researchers report a decrease in the dynamics of water in a hydration shell, which is several times or even several orders of magnitude smaller than that of the bulk water [21]. However, several simulations [22, 23] have determined the parameters of nanoparticles which may accelerate the dynamics of water, making it even faster than the dynamics of bulk water.

A number of studies have investigated the water dynamics in the near-surface layer for molecules or nanoparticles with varying degree of hydrophobicity–hydrophilicity [24, 25, 26]. An interesting result is that the relaxation time of confined water may be less than that of bulk water in the case of hydrophilic hydration [24]. In the framework of these studies, the cellulose nanoparticles are attractive due to their chemical flexibility: originally the surface is hydrophobic, but chemical modification of hydrogen bonds can increase hydrophobic properties of the surface [27, 28].

The investigation of the aqueous suspensions of cellu-

This work may be used under the terms of the Creative Commons Attribution 4.0 International License. Further distribution of this work must maintain attribution to the author(s) and the title of the paper, journal citation, and DOI.

lose nanoparticles may be useful for application in modern technologies; besides, it is interesting from the point of view of fundamental research due to its relation to the understanding of relaxation mechanisms. Two types of nanoparticles were used in our study, cellulose nanocrystals and cellulose nanofibers. These nanoparticles differ not only in morphology but also in the chemical structure of the surface: on the surface of the nanocrystals, there are additional hydrophilic functional groups, which create favourable conditions increasing the dynamics of water molecules near its surface. As a result, the relaxation time of the water–cellulose nanocrystals suspension is less than the relaxation time of water or the water–cellulose nanofibers suspension.

II. EXPERIMENTAL SECTION

Materials. Soft wood pulp (International Paper at Flint River Mill, USA) was used for isolation of the nanocellulose. Sulphuric acid (95–98%) and sodium bromide were purchased from Sigma-Aldrich. The Ultrapure water used in all the experiments was prepared in a three-stage Millipore Milli-Q Plus 185 purification system (resistivity $\geq$18.2 MΩ·cm).

Extraction of nanocellulose. The CNCs were isolated by the common sulphuric acid hydrolysis method [29]. Briefly, the hydrolysis was performed using 64% w/w sulphuric acid (H_2SO_4) at 45±0.5°C. The cellulose source to acid ratio is 5 g to 95 g. The time of the hydrolysis is 60 min. The remaining sulphuric acid was removed by dialysis until pH neutrality was reached. The CNFs were isolated through the common TEMPO oxidation method. [30]. Briefly, TEMPO (0.016 g, 0.1 mmol) and sodium bromide (0.1 g, 1 mmol) were added into 1 wt.% wood pulp suspension. Then the NaClO solution (12%, 10 mmol NaClO to 1 gram of cellulose) was added to the above mixture at stirring (500 rpm). The TEMPO-oxidized wood pulp was thoroughly washed with water and then treated by an ultrasonic tip for 2 h. High-speed centrifugation (10000 rpm, 20 min, 5°C) was conducted to separate the cellulose nanofiber suspension.

Characterization. The chemical composition of the cellulose nanoparticles was studied by Fourier transform infrared (FTIR) and Energy-dispersive X-ray (EDX) spectroscopy. The FTIR spectra were conducted using a Bruker Vertex 70 FTIR spectrophotometer operated in 200–4500 cm^{-1} range. The EDX spectroscopy was performed with an Oxford EDX attached to a scanning electron microscope operating at 5 kV with a live time of 1200 s.

The dielectric properties of the aqueous suspensions were investigated by Keysight Network Analyzer N5227A with Agilent Dielectric Probe sensor in the frequency range of 1 GHz to 30 GHz at temperatures of 22, 32, 42°C.

III. RESULTS AND DISCUSSION

Nanocellulose Chemical Composition. The EDX was used for the elemental analysis of CNC and CNF. The EDX spectra showed two peaks corresponding to main cellulose components, carbon (C) and oxygen (O) (Fig. 1). Also, we observe elemental impurity of sulphur (S) in CNCs and sodium (Na) in CNFs. These impurities are due to the isolation process.

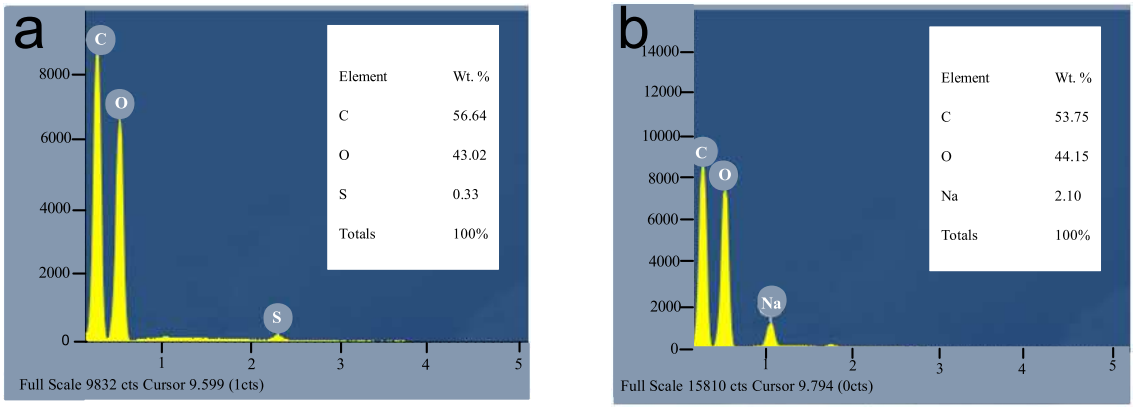

Fig. 1. The EDX spectra and element distribution of the CNCs (a) and CNFs (b)

The amount of carbon and oxygen in a cellulose chain $(C_6H_{10}O_5)$n should be 54.55 at.% (47.37 wt.%) and 45.45at.% (52.63 wt.%) respectively. The elemental distribution of the CNCs and the CNFs deviates from that of the cellulose chain; however, it is in good agreement with literature data [31, 32].

The FTIR spectra of the CNCs and the CNFs were analyzed to understand molecular structure and structural changes in both samples (Fig. 2). The interpretation of bands is given in Table 1. Bands of the CNCs in the range of 3600–3100 cm^{-1} are shifted to higher wavenumbers comparing to corresponding bands of the CNFs. The shift to higher wavenumbers might be due to the average decrease in hydrogen bonds strength [33] or hydrogen bonds destruction [34].

Bonds	Wavenumber, cm^{-1}	
	CNCs	CNFs
O(2)H...O(6) bond vibration [36]	3446	
O(3)–H...O(5) [37]	3375	
C–H stretching	2901	2901
C=O bond stretching [38], [33]	1758-1692	1741
C=O stretching [39]	1673	
C=C aromatic skeletal vibration and C=O stretching [33]	1608	1607
C–H bending C–H [33]	1427, 1372, 1362, 1356	1421, 1372
C–O stretching and C–H bending [33]	1280	
O–H in-plane bending [33]	1204	
C–O–C asymmetric vibration [33]	1164	1162
Ring asymmetric stretching [34].		1111
C–O valence vibration [39].		1061
C–O stretching [40]	1000	
C–H wagging [33]	898	
C–H out of plane bending [39]	859	
O–H out of plane bending [33], [40]	704, 666	

Table 1. Vibration type and corresponding wavenumber for the CNCs and the CNFs.

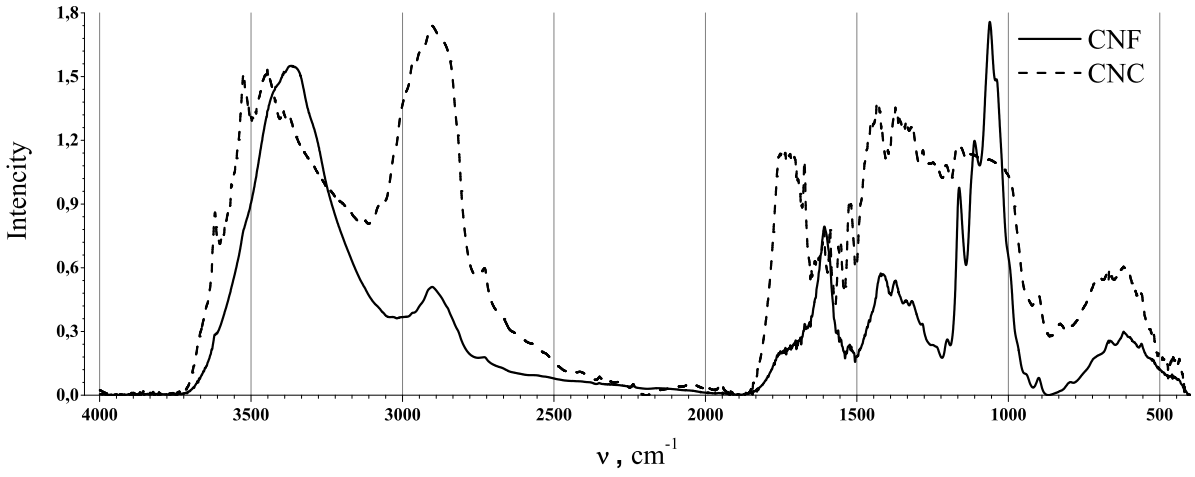

Fig. 2. The FTIR spectra of the CNCs and the CNFs

The intensity of the bands corresponding to C=O bonds stretch (1750–1600 cm^{-1}) is higher for the CNCs than for the CNFs, however, for the CNCs these bands must be absent [34]. The appearance of the intense bands in this range may be due to cellulose partial oxidation [35]. When oxidizing C–H, C–OH, C–C bonds may be destroyed with the formation of the C=O bonds. The characteristic wavenumbers of newly formed bonds, as determined in [36], are 1745, 1732, 1713, 1685, 1665, 1617 cm^{-1}.

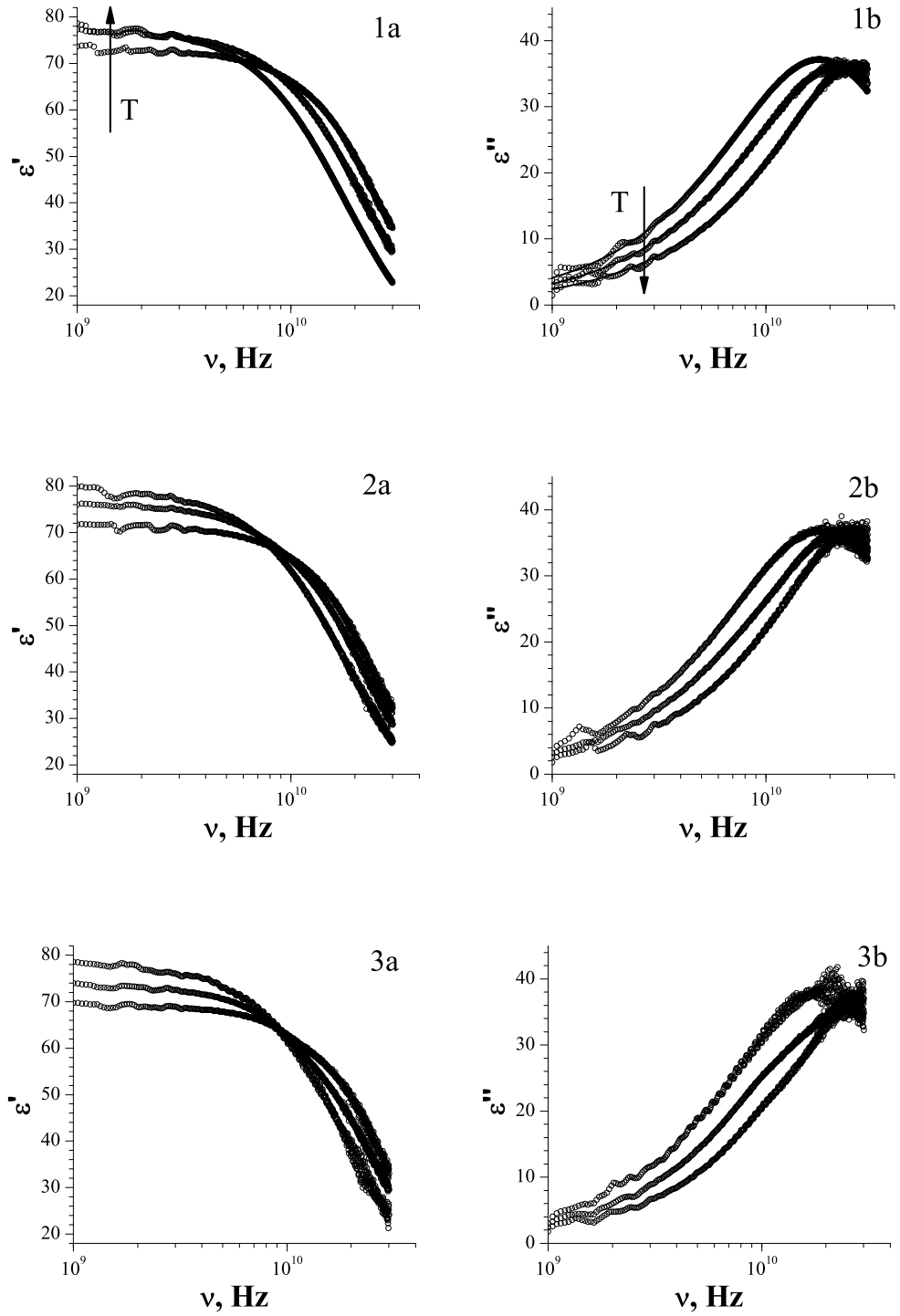

Fig. 3. The frequency dependence of the real ε' (a) and imaginary ε'' (b) part of permittivity for the water (1), the water–CNCs suspension (2), and the water–CNFs suspension (3) with temperature change

Bands 1608 cm^{-1} of the CNCs and 1607 cm^{-1} of the CNFs may correspond to the C=O bonds stretch or C=C bonds vibrations. However, as mentioned before, the C=O bonds are not typical of the CNCs. Besides, the C=C bonds can be observed for wood materials but not for the CNCs. The presence of this band can be explained by the presence of functional groups in the CNCs.

The band 1062 cm^{-1} corresponding to C–O bonds vibrations becomes smoother for the CNCs comparing to the CNFs. The C–O bonds are present in the glucose ring, between glucose rings and between skeleton atoms and OH groups. Due to the oxidation of the OH groups injected to C atoms, the OH groups can be replaced with functional groups having the C=O bonds. This explains the

intensity decrease of 1062 cm^{-1} band and agrees with the band intensity increase in the range of 1700–1600 cm^{-1}.

IV. DIELECTRIC PROPERTIES OF CNCS AND CNF IN AQUEOUS MEDIA

The dielectric properties are measured to investigate relaxation of liquid systems with hydrogen bonds [41]. Permittivity, ε, is complex, so it can be presented as follows:

$$\varepsilon = \varepsilon' - i\varepsilon'' \tag{1}$$

where ε' the real part related to the stored energy within the medium, ε'' the imaginary part related to the dissipation of energy within the medium, i is the imaginary unit.

The permittivity of water is described by the Debye model in the investigated range of frequencies (1 GHz to 30 GHz) [42, 43, 44]. Appart from the Debye model, there are more complex models having more parameters accounting for the asymmetry and broadness of the dielectric dispersion curve [45]: Cole–Cole, Davidson–Cole, Williams–Wats, Havriliak–Negami, Jonsher, Dissado Hill. In our case, it is necessary to use the Debye model, because a greater number of parameters introduces uncertainty into the curve behaviour description, or simplifies to the Debye model when approximating.

According to the Debye model, the frequency dependence of permittivity is given as follows:

$$\varepsilon(\nu) = \varepsilon'(\nu) - i\varepsilon''(\nu) = \varepsilon_\infty + \frac{\varepsilon_0 - \varepsilon_\infty}{1 + 2\pi i\nu\tau} \tag{2}$$

where ν is the frequency of electromagnetic field, ε_∞ is the value of dielectric permittivity at $\nu \to \infty$, ε_0 is the value of dielectric permittivity at $\nu \to 0$, and τ is the characteristic relaxation time.

The real and the imaginary permittivity are derived from equation (2) as follows:

$$\varepsilon'(\nu) = \varepsilon_\infty + \frac{\varepsilon_0 - \varepsilon_\infty}{1 + (2\pi\nu\tau)^2} \tag{3}$$

$$\varepsilon''(\nu) = \frac{2\pi\nu\tau(\varepsilon_0 - \varepsilon_\infty)}{1 + (2\pi\nu\tau)^2}. \tag{4}$$

Equation (4) provides unequivocal values of parameters ($\varepsilon_0 - \varepsilon_\infty$, τ), unlike equation (3), where parameters (ε_0, ε_∞, τ) are mutually dependent. Equation (4) was used to determine the relaxation time τ.

Tempera–ture,°C	Literature data [17]		Debye		Cole–Cole			Davidson–Cole		
	$\varepsilon_0 - \varepsilon_\infty$	τ, 10^{-12}s	$\varepsilon_0 - \varepsilon_\infty$	τ, 10^{-12}s	$\varepsilon_0 - \varepsilon_\infty$	τ, 10^{-12}s	α	$\varepsilon_0 - \varepsilon_\infty$	τ, 10^{-12}s	β
22	73.88	8.92	74.19	8.91	74.15	8.91	0	73.98	8.90	1
32	70.52	6.97	71.95	7.25	71.95	7.26	0	73.75	7.25	0.97
42	67.4	5.61	72.74	5.48	72.73	5.49	0	73.46	5.49	0.98

Table 2. The parameters for water.

The parameters for water of the Debye, Cole–Cole and Davidson–Cole equations and the comparison with the literature data are shown in Table 2. In the case of the Cole–Cole model, an extra parameter α takes zero value, which means the equation simplifies to the Debye model. In the case of the Davidson–Cole model, the parameter β slightly differs from the unit, making the equation different from the Debye one. The Davidson–Cole equation has four parameters, as a result, an uncertainty appears, the range of values of ε_0 providing an appropriate approximation ($\chi^2 < 1$) extends by about four times if compared to the same parameter of the Debye equation; however, the errors in other parameters of these equations are comparable. On the basis of these results, it is decided to use the Debye equation for the analysis.

The values of the parameter $\varepsilon_0 - \varepsilon_\infty$ at the temperatures of 22 and 32°C differ from the literature data by 0.2%, however, at the temperature of 42°C the deviation is 8% [17]. The deviation at 42°C may be explained by a dynamic phase transition in pure water [46]. The authors of work [46] claim the existence of two states of water; the first one, below 42°C, is characterized by the crystal-like character of the thermal motion, the second one, for the temperatures higher than 42°C, is characterized by the thermal motion tending to the argon-like type.

A linear approximation was used to determine the values of ε_0, ε_∞ and τ from literature data at given temperatures [17]. The values of ε_∞ at the temperature of 40°C [47] are less than at 35 or 50°C, so it can be presumed that at the temperature of 42°C the parameter ε_∞ has a minimum. In this case, the difference ε_0-ε_∞ at 42°C is greater than it was expected. The relaxation time deviates from literature data by 6%.

The values of the parameters ε_0, ε_∞ and τ were also determined for the aqueous suspensions of the CNCs and the CNFs (Table 3).

Sample	Temperature,°C	$\varepsilon_0 - \varepsilon_\infty$	τ, 10^{-12}s
Water–CNCs	22	76.24	8.24
	32	70.15	6.59
	42	76.95	4.51
Water–CNFs	22	73.73	8.77
	32	71.81	7.07
	42	73.73	5.42

Table 3. The parameters for the aqueous CNCs and CNFs suspensions.

The relaxation time decreases with the temperature increase for all samples (Fig. 4). This can be explained by the fact that the loss factor decreases with increasing temperature at high frequencies due to free-water dispersion [48]. This decrease agrees with the results of other works [49, 50].

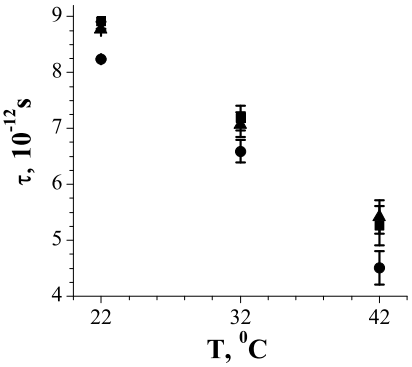

Fig. 4. The temperature dependence of the relaxation time for water (■), the water-CNCs suspension (▲) and water-CNFs suspension (●).

The relaxation time of the water–CNCs suspension is significantly smoller (7.5% less at 22°C) than that of the water, while the relaxation time of the water–CNFs suspension has a smaller deviation (1.6% less at 22°C).

The characteristic relaxation time depends on the time required to reorient the dipole and the lifetime of the hydrogen bond [17]. The time for the reorientation of the molecule depends on the number of its neighbours: a larger number of neighbour molecules makes it possible to create a new hydrogen bond faster. In addition, the lifetime of a hydrogen bond depends on the activation energy for water rotation, which depends on external fields. In order to explain the difference in the time of relaxation of the investigated systems, it is necessary to consider the factors that could change the above parameters.

Cellulose nanoparticles have hydrophilic properties [51]. The results of the FTIR spectrum analysis indicate the presence of additional hydrophilic functional groups on the surface of the CNCs. The CNCs and the CNFs surfaces have distinct wall potentials. The nanoparticle wall potential is the external field causing changes in the structure of the water layer near the surface, causing changes in the water relaxation time.

In paper [22], the authors have studied the dependence of the confined water dynamics on the hydrophobic/hydrophilic properties of the surface. It has been determined that the surface with hydrophobic or very hydrophilic properties slows down the dynamics of water molecules, but there is the surface hydrophilicity level having the minimum slowdown, a 1.2 decrease comparing to bulk water.

In the paper [24], the authors have investigated the dielectric relaxation in hydration shells of ions. It is shown that for the ions with hydrophobic hydration there is a good complementary organization of the hydration shells and bulk water; as a result, the relaxation time of the solutions is greater than the water relaxation time. In the case of hydrophilic hydration, two variants of structural and geometric changes in the hydration layer of the ions can be realized: the characteristic relaxation time of solutions can be greater or less than the characteristic relaxation time of water. Other papers [25, 26] have also shown the existence of two possible variants of water relaxation time behaviour nearby the surface of ions with hydrophilic properties.

Based on these studies, it can be assumed that the relaxation time decrease in the water–CNCs suspension is due to the hydrophilic properties of the CNCs surface. The structure of water near the surface of the nanocrystals allows water molecules to find a molecule to create a new bond faster. The rotational energy barrier of water molecules influenced by CNCs is less than that of bulk water molecules.

V. CONCLUSION

The dielectric properties of the water suspensions of cellulose nanoparticles were studied. Based on the EDX and the FTIR investigation, the presence of additional hydrophilic functional groups on the CNCs surface is assumed; the CNFs do not exhibit unusual features in their structure. The impurity of the CNFs insignificantly ($> 1\%$) changes the dielectric properties of the water suspension in the frequency range of 1 to 30 GHz; however, the impurity of the CNCs makes has a greater effect (3%). This tendency is observed at the temperatures of 22, 32 and 42°C. The decrease in the relaxation time of the water–CNCs suspension is explained by the features of the CNCs surface, allowing the increase in the water molecules dynamics in the near-wall layer, consequently affecting the relaxation behaviour of all system.

VI. ACKNOWLEDGMENTS

Authors thank Dr Volodymyr F. Korolovych and Prof. Vladimir Tsukruk (Georgia Institute of Technology) for their help with the measurements and technical assistance.

[1] T. Abitbol *et al.*, Curr. Opin. Biotechnol. **39**, 76 (2016).
[2] X. Du, Z. Zhang, W. Liu, Y. Deng, Nano Energy **35**, 299 (2017).
[3] Y. Zhao, C. Moser, M. E. Lindstrom, G. Henriksson, J. Li, ACS Appl. Mater. Interfaces. **9**, 13508 (2017).
[4] M. Giese, L. K. Blusch, M. K. Khan, W. Y. Hamad,

M. J. Maclachlan, Angew. Chem. Int. Ed. **53**, 8880 (2014).
[5] Y. Wu *et al.*, Food Chem. **197**, 250 (2016).
[6] N. Noshirvani *et al.*, Food Hydrocoll. **70**, 36 (2017).
[7] C. Ye, S.T. Malak, K. Hu, W. Wu, V. V. Tsukruk, ACS Nano **9**, 10887 (2015).
[8] T. Paulraj *et al.*, Bioinsipired. **18**, 1401 (2017).
[9] Y. Yoo, C. Martinez, J. P. Youngblood, Langmuir **33**, 1521 (2017).
[10] Y. Ono, T. Shikata, J. Am. Chem. Soc. **128**,10030 (2006).
[11] B. Bagchi, Water, Chem. Rev. **105**, 3197 (2005).
[12] L. Comez *et al.*, Soft Matter **12**, 5501 (2016).
[13] D. Laage, T. Elsaesser, J. T. Hynes, Chem. Rev. **117**, 10694 (2017).
[14] S.K. Pal, J. Peon, B. Bagchi, A.H. Zewail, J. Phys. Chem. B **106**, 12376 (2002).
[15] Y. Feldman, Y. A. Gusev, M. A. Vasilyeva, *Dielectric Relaxation Phenomena in Complex Systems: Tutorial* (The Kazan Federal University, Institute of Physics, 2012).
[16] R. Buchner, Pure Appl. Chem. **80**, 1239 (2008).
[17] P. Petong, R. Pottel, U. Kaatze, J. Phys. Chem. A **104**, 7420 (2000).
[18] R. K. Murarka, T. Head-Gordon, J. Phys. Chem. B **112**, 179 (2008).
[19] C. Cametti, S. Marchetti, C. M. C. Gambi, G. Onori, J. Phys. Chem. B **115**, 7144 (2011).
[20] C. Cametti, I. Fratoddi, I. Venditti, M. V Russo, Langmuir **27**, 7084 (2011).
[21] F. Pizzitutti, M. Marchi, F. Sterpone, P. J. Rossky, J. Phys. Chem. B. **111**, 7584 (2007).
[22] G. Stirnemann *et al.*, Phys. Chem. Chem. Phys. **13**, 19911 (2011).
[23] S. Roy, B. Bagchi, J. Phys. Chem. B. **116**, 2958 (2012).
[24] A. Lyashchenko, A. Lileev, J. Chem. Eng. Data **55**, 2008 (2010).
[25] P. S. Yastremskii *et al.*, Zh. Fiz. Khim. **46**, 1442 (1975).
[26] P. S. Yastremskii, G. V. Kokovina, A. K. Lyashchenko, Y. A. Mirgorod, J. Struct. Chem. **16**, 921 (1975).
[27] M. A. Hubbe, O. J. Rojas, L. A. Lucia, M. Sain, BioResources **3**, 929 (2008).
[28] Y. Habibi, L. A. Lucia, O. J. Rojas, Chem. Rev. **110**, 3479 (2010).
[29] V. F. Korolovych *et al.*, Polymer (Guildf) **145**, 334 (2018).
[30] R. Xiong *et al.*, ACS Nano **11**, 12008 (2017).
[31] Z. Man *et al.*, J. Polym. Environ. **19** 726 (2011).
[32] A. Kumar, Y. S. Negi, V. Choudhary, N. K. Bhardwaj, J. Mater. Phys. Chem. **2**, 1 (2014).
[33] M. Le Normand, R. Moriana, M. Ek, Carbohydr. Polym. **111**, 979 (2014).
[34] T. Steinel, J. B. Asbury, J. R. Zheng, M. D. Fayer, J. Phys. Chem. A **108**, 10957 (2004).
[35] J. Lojewska, P. Miskowiec, T. Lojewski, L. M. Proniewicz, Polym. Degrad. Stab. **88**, 512 (2005).
[36] M. Fan, D. Dai, B. Huang, in *Fourier Transform–Materials Analysis. Ch. 3*, edited by S. M. Salih (InTech Press, 2012).
[37] T. Kondo, Cellulose, **4**, 281 (1997).
[38] K. K. Pandey, J. Appl. Polym. Sci. **71**, 1969 (1999).
[39] M. Schwanninger, J.C. Rodrigues, H. Pereira, B. Hinterstoisser, Vib. Spectrosc. **36**, 23 (2004).
[40] F. G. Pearson, C. Y. Liang, R. H. Marchessault, J. Polym. Sci. **43**, 101 (1960).
[41] G. Z. Jia, F. Wang, X. Q. Yang, J. Qian, J. Mol. Liq. **197**, 328 (2014).
[42] H. J. Liebe, G. A. Hufford, T. Manabe, Int. J. Infrared Millim. Waves **12**, 659 (1991).
[43] V. G. Artemov, I. A. Ryzhkin, V. V. Sinitsyn, JETP Lett. **102**, 41 (2015).
[44] N. V. Chekalin, M. I. Shakhparonov, J. Struct. Chem. **9**, 145 (1968).
[45] J. Macutkevic, J. Banys, A. Matulis, Nonlinear Anal. Model. Control. **9**, 75 (2004).
[46] L. A. Bulavin, A. I. Fisenko, N. P. Malomuzh, arXiv: 1307.7295 (2013).
[47] U. Kaatze, J. Chem. Eng. Data. **34**, 371 (1989).
[48] V. Komarov, S. Wang, J. Tang, Encycl. RF Microw. Eng. **47**, 2123 (1999).
[49] R. Buchner, J. Barthel, J. Stauber, Chem. Phys. Lett. **306**, 57 (1999).
[50] J. Hunger, A. Stoppa, S. Schrodle, G. Hefter, R. Buchner, Chem. Phys. Chem. **10**, 723 (2009).
[51] J. Lu, P. Askeland, L. T. Drzal, Polymer (Guildf) **49**, 1285 (2008).

ДІЕЛЕКТРИЧНІ ВЛАСТИВОСТІ ВОДНИХ СУМІШЕЙ ІЗ НАНОКРИСТАЛАМИ ТА НАНОВОЛОКНАМИ ЦЕЛЮЛОЗИ

Олег Гребньов*, Людмила Мацуй, Леонід Булавін
Київський національний університет імені Тараса Шевченка,
вул. Володимирська, 64, Київ, 01601, Україна
**e-mail: orticort@gmail.com*

Діелектричні властивості водних сумішей із наночастинками з гідрофобними властивостями інтенсивно досліджують у нас час. Проте небагато робіт присвячено вивченню суміші з гідрофільними наночастинками. У цій статті досліджено вплив гідрофільних нанокристалів та нановолокон целюлози на діелектричні властивості водних сумішей. Чистота та хімічний склад наночастинок охарактеризовано EDX- та FTIR-сектроскопією. Результати діелектричних вимірювань показали зменшення часу релаксації у водних сумішах із нанокристалами целюлози порівняно з часом релаксації води; не виявлено значної зміни часу релаксації у водних сумішах із нановолокнами целюлози. Результати дослідження вказують на те, що гідрофільна поверхня може прискорювати динаміку молекул води.